DOI: 10.1002/ejic.200600570

Oxalato-Bridged Dinuclear Copper(II) Complexes of *N*-Alkylated Derivatives of 1,4,7-Triazacyclononane: Synthesis, X-ray Crystal Structures and Magnetic Properties

Matthew J. Belousoff,[a] Bim Graham,[a][‡] Boujemaa Moubaraki,[a] Keith S. Murray,[a] and Leone Spiccia*[a]

Keywords: Dinuclear copper(II) complexes / Oxalato bridges / *N*-Alkylated 1,4,7-triazacyclononane derivatives / X-ray structures / Antiferromagnetic coupling

The synthesis, X-ray crystal structure and magnetic properties of two oxalato-bridged dinuclear Cu^{II} complexes, [L-Cu(μ-ox)Cu-L](ClO$_4$)$_2$, where ox = oxalate and L = 1,4,7-trimethyl-1,4,7-triazacyclononane (Me$_3$tacn) or 1-benzyl-4,7-dimethyl-1,4,7-triazacyclononane (BzMe$_2$tacn) are reported, as well as the X-ray crystal structure of the mononuclear complex, [Cu(Me$_3$tacn)(OH$_2$)$_2$](ClO$_4$)$_2$, which features an extended H-bonding network between the ligand and the perchlorate counterions. The crystal structures of the dinuclear complexes both feature a centrosymmetric complex cation in which the two copper centres exist in a distorted square-pyramidal geometry, with each end capped by a facially coordinated "tacn" unit, and are bridged by an oxalate anion. Variable-temperature magnetic susceptibility measurements revealed strong antiferromagnetic interactions between the Cu^{II} centres, with 2*J* values of ca. –300 cm^{-1}, even though the Cu···Cu separation is very long, viz. 5.18 Å (BzMe$_2$tacn) and 5.47 Å (Me$_3$tacn). The separation for the Me$_3$tacn complex is the longest separation reported for this type of Cu^{II} complex. No pattern could be detected between the *J* values and structural features for 21 oxalato-bridged complexes.

Introduction

The magnetic properties of copper(II) complexes have been an attractive area of research. This is due to the fact that copper(II) (d^9) has a single unpaired electron and therefore can be used as a model system for probing the nature of magnetic exchange interactions between single unpaired electrons on two or more metal centres, and, in particular, how this interaction is mediated by the ligands that bridge the metal centres.[1–3] Hydroxo-bridged metal complexes, in which the metal atoms are linked by single-atom bridges, have been most widely studied. The data that have been obtained have been used to develop empirical correlations of the strength of magnetic coupling with key structural descriptors of the Cu–OH–Cu bridging unit(s).[4–6] Further, theoretical analyses have been undertaken in an effort to develop a molecular orbital view of coupling in these complexes.[7,8]

Oxalato-bridged complexes have also been of interest[9–15] since, in this case, the Cu^{II} centres are linked by multi-atom bridges, yet they can exhibit quite strong antiferromagnetic interactions even when the Cu^{II} centres are separated by more than 5 Å.[2] Whilst most of these complexes exhibit antiferromagnetic coupling, the strength of this interaction can vary from very weak [2*J* value (exchange constant) close to 0 cm^{-1}] to very strong (2*J* value up to –400 cm^{-1}). The strength of the antiferromagnetic interaction has been proposed to be related to the "square of the overlap between the magnetic orbitals located on each copper(II)".[1] In the case of the oxalato-bridged copper(II) complexes it is the overlap of the d$_{x^2-y^2}$ and the σ-bonding orbitals on the oxygen atoms of the oxalato bridge that determines the strength of the interaction.

The ligand 1,4,7-triazacyclonone (tacn) is a particularly well-studied aza-macrocycle that uses three N-donor atoms to bind to the copper atom, forming highly stable complexes. Copper(II)–tacn complexes exhibit well-defined coordination polyhedra, consistently adopting either distorted octahedral or square-pyramidal geometries. The proposal by Kahn et al. that the extent of spin coupling in dinuclear complexes could be "tuned" by changing the Cu^{II} coordination sphere that supports the oxalato bridge[1] led us to investigate the effect of geometric constraints introduced by the tacn macrocycle on the extent of magnetic interaction between the metal centres in oxalato-bridged dinuclear copper(II) complexes. Herein we report the synthesis, X-ray crystal structure and magnetic properties of two new oxalato-bridged copper(II) complexes of *N*-alkylated tacn

---

[a] School of Chemistry, Monash University,
Victoria, 3800, Australia
Fax: +61-3-99054597
E-mail: leone.spiccia@sci.monash.edu.au
[‡] Current address: Department of Medicinal Chemistry,
Victorian College of Pharmacy, Monash University,
381 Royal Parade, Parkville, Victoria, 3052, Australia

macrocycles (Me_3tacn = 1,4,7-trimethyl-1,4,7-triazacyclononane and $BzMe_2$tacn = 1-benzyl-4,7-dimethyl-1,4,7-triazacyclononane) and, for comparison, the X-ray crystal structure of $[Cu(Me_3tacn)(OH_2)_2](ClO_4)_2$ (**C1**).

Results and Discussion

$[Cu_2(Me_3tacn)(\mu\text{-ox})](ClO_4)_2$ (**C2**) was prepared by treating the diaqua mononuclear precursor, $[Cu(Me_3tacn)(OH_2)_2](ClO_4)_2$ (**C1**),[16] with 1 equiv. of sodium oxalate (see Scheme 1). Careful concentration of the solution to dryness and recrystallisation from a mixture of methanol/ethanol (1:1) produced analytically pure blue crystals. The IR spectrum of **C2** reveals the characteristic stretching modes of the oxalato ligand at 1648 cm^{-1} (υ_{asym}) and 1467 cm^{-1} (υ_{sym}), which are typical for bridging oxalato ligands.[17] The solution UV/Vis spectrum shows the electronic d→d transitions expected for square-pyramidal copper(II) complexes at 1100 nm (ε_{max} = 68 $M^{-1} cm^{-1}$) and 636 nm (ε_{max} = 118 $M^{-1} cm^{-1}$).[18] Band maxima are also observed at 333 nm (ε_{max} = 4160 $M^{-1} cm^{-1}$), 282 nm (ε_{max} = 11100 $M^{-1} cm^{-1}$) and 195 nm (ε_{max} = 11400 $M^{-1} cm^{-1}$), which could result from either charge transfer or ligand $\pi \rightarrow \pi^*$ transitions.

The synthesis of $[Cu_2(BzMe_2tacn)(\mu\text{-ox})](ClO_4)_2$ (**C3**) involved first the formation of the precursor mononuclear copper(II) complex in an aqueous methanolic solution, which was then treated with sodium oxalate to yield the desired dinuclear complex as analytically pure blue crystals (see Scheme 1). The IR spectrum of **C3** again shows the expected stretching modes from the oxalato ligand at 1654 cm^{-1} (υ_{asym}) and 1466 cm^{-1} (υ_{sym}). The electronic spectrum exhibits two d→d transitions at 1090 nm (ε_{max} = 67 $M^{-1} cm^{-1}$) and 644 nm (ε_{max} = 110 $M^{-1} cm^{-1}$), which again suggests that the copper(II) centre exists in a square-pyramidal geometry in solution.[18] A strong band at 284 nm (ε_{max} = 9100 $M^{-1} cm^{-1}$) could be an MLCT or a $\pi \rightarrow \pi^*$ transition within the ligand.

X-ray Crystal Structure Determinations

The X-ray crystal structure of **C1** reveals a mononuclear complex, in which the distorted octahedral copper(II) coordination sphere is occupied by three nitrogen donors from the Me_3tacn ligand, two oxygen atoms from ligated water and a distant oxygen atom from a perchlorate counteranion (see Figure 1). There is significant elongation in the axial direction of the coordination polyhedron, viz. the Cu(1)–N(1) bond is 0.19 Å longer than the Cu–N distances in the basal plane and for the weakly interacting perchlorate anion the Cu(1)–O(1) distance is 2.519(3) Å. All other bond lengths and angles are in the expected range for (tacn)Cu^{II} complexes (see Table 1).

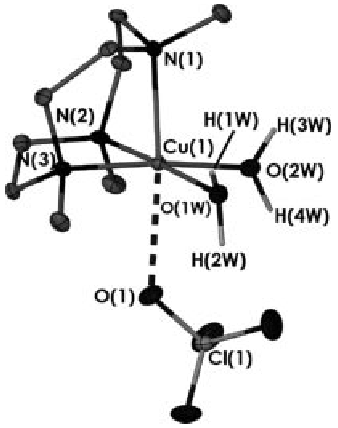

Figure 1. Thermal ellipsoid plot of **C1** (drawn at 50% probability). Dashed line indicates a weak interaction; some hydrogen atoms and a perchlorate anion have been omitted for clarity.

The hydrogen-bonding network formed by the hydrogen atoms from the coordinated water molecules and the perchlorate anions is particularly interesting. Each coordinated water molecule hydrogen-bonds to different perchlorate anions, which in turn hydrogen-bond to water molecules coordinated to different complexes (Table 2). This forms infinite two-dimensional layered sheets (see Figure 2).

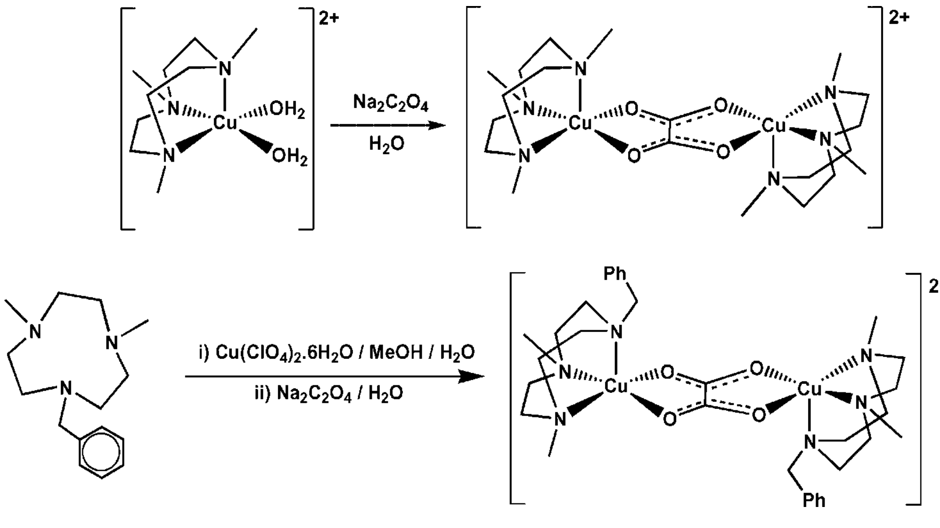

Scheme 1. Synthesis of oxalato-bridged copper(II) complexes.

Table 1. Selected bond lengths [Å] and angles [°] for **C1** (esd in parentheses).

Cu(1)–O(1W)	2.004(2)	O(1W)–Cu(1)–N(2)	176.56(8)
Cu(1)–N(2)	2.031(2)	O(1W)–Cu(1)–O(2W)	85.98(8)
Cu(1)–O(2W)	2.044(2)	N(2)–Cu(1)–O(2W)	92.24(9)
Cu(1)–N(3)	2.063(2)	O(1W)–Cu(1)–N(3)	95.42(8)
Cu(1)–N(1)	2.218(2)	N(2)–Cu(1)–N(3)	86.02(8)
Cu(1)–O(1)	2.519(3)	O(2W)–Cu(1)–N(3)	173.53(8)
		O(1W)–Cu(1)–N(1)	98.24(8)
		N(2)–Cu(1)–N(1)	84.98(8)
		O(2W)–Cu(1)–N(1)	101.06(8)
		N(3)–Cu(1)–N(1)	85.01(8)

Table 2. Hydrogen bonds for **C1** [Å and °] (esd in parentheses).

D–H···A	d(D–H)	d(H···A)	d(D···A)	<(DHA)
O(2W)–H(3W)···O(6)[a]	0.93(1)	1.84(1)	2.760(3)	167(3)
O(1W)–H(1W)···O(7)[b]	0.94(1)	1.85(2)	2.749(3)	159(3)
O(2W)–H(4W)···O(2)[c]	0.93(1)	2.12(2)	2.919(3)	144(3)
O(2W)–H(4W)···O(4)	0.93(1)	2.50(3)	3.108(3)	123(3)
O(1W)–H(2W)···O(3)[d]	0.93(1)	1.97(3)	2.729(3)	137(4)
O(1W)–H(2W)···O(4)	0.94(1)	2.62(4)	3.219(3)	122(3)

Symmetry transformations used to generate equivalent atoms: [a] $-x, -y + 1, -z + 1$. [b] $-x + 1, -y + 1, -z + 1$. [c] $-x, -y + 1, -z + 2$. [d] $-x + 1, -y + 1, -z + 2$.

The structure of **C2**, shown in Figure 3, reveals a dinuclear copper(II) complex featuring two capping Me_3tacn ligands and a bridging oxalato ligand that binds through all four of its oxygen atom. The complex is centrosymmetric, half existing in the asymmetric unit (ASU), with the other half generated by crystallographic symmetry. The metal centres at each end of the complex exist in a highly distorted geometry because of the geometric constraints introduced by the tacn macrocycle and the bridging oxalato ligand (see Table 3). The degree of distortion is highlighted by the three quite different Cu–N distances, which, in a five-coordinate complex, would be indicative of distortion away from square-pyramidal towards trigonal-bipyramidal geometry. An oxygen atom from a perchlorate anion is oriented in the direction of the vacant axial position of the copper(II) coordination polyhedron [Cu–O distance of 2.808(5) Å]. This distance is much longer than that in **C1**, probably because of the distortion of the coordination polyhedron beyond the usual tetragonal elongation. Whether the solid-state Cu^{II} geometry is best described as distorted octahedral (6-coordinate) or distorted square-pyramidal (5-coordinate) is therefore debatable. With respect to the oxalato bridge, the two apical tacn nitrogen atoms in each dinuclear complex adopt a *trans* configuration. The two copper

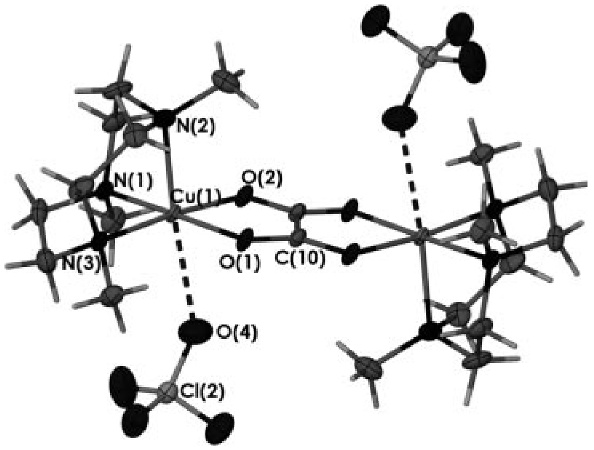

Figure 3. Thermal ellipsoid plot of **C2** (drawn at 50% probability). Dashed lines indicate a weak coordination bond.

Table 3. Selected bond lengths [Å] and angles [°] for **C2** (esd in parentheses).

Cu(1)···Cu(1)[a]	5.467(3)	O(1)–Cu(1)–N(1)	175.7(1)
Cu(1)–O(1)	2.026(2)	O(1)–Cu(1)–O(2)	81.3(1)
Cu(1)–O(2)	2.091(2)	N(1)–Cu(1)–O(2)	95.4(1)
Cu(1)–N(1)	2.052(3)	O(1)–Cu(1)–N(3)	99.5(1)
Cu(1)–N(3)	2.141(3)	N(1)–Cu(1)–N(3)	83.4(1)
Cu(1)–N(2)	2.248(3)	O(2)–Cu(1)–N(3)	173.6(1)
Cu(1)–O(4)	2.808(5)	O(1)–Cu(1)–N(2)	96.9(1)
O(1)–C(10)	1.316(4)	N(1)–Cu(1)–N(2)	86.3(1)
O(2)–C(10)[a]	1.289(4)	O(2)–Cu(1)–N(2)	97.5(1)
C(10)–O(2)[a]	1.289(4)	N(3)–Cu(1)–N(2)	88.7(1)
C(10)–C(10)[a]	1.554(6)		

Symmetry transformations used to generate equivalent atoms: [a] $-x + 1/2, -y + 1/2, -z$.

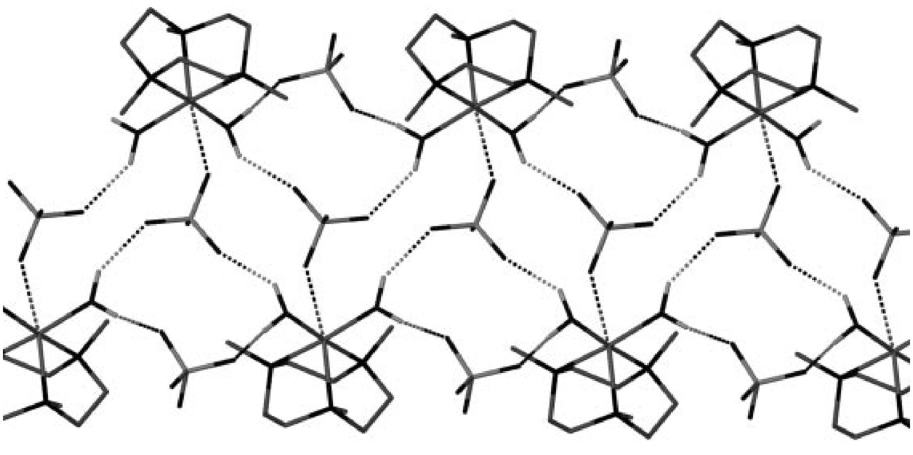

Figure 2. Infinite two-dimensional sheets formed by hydrogen-bonding interactions (dotted lines) in **C1**.

atoms are separated by 5.467(3) Å, and the Cu–O(ox) distances of 2.026(2) and 2.091(2) Å indicate that the two pairs of stronger and weaker binding oxygen atoms adopt a *trans* configuration.

A least-squares analysis of the plane of the oxalato ligand and the O(1)–Cu(1)–O(2) plane reveals that the CuN_2O_2 basal unit does not lie in the same plane as the oxalato ligand (see Figure 7). The dihedral angle created by the intersection of these two planes [φ = 4.8(3)°] means that there is a "step" between the two coordination spheres, perhaps reducing the overlap of the $d_{x^2-y^2}$ and the σ-bonding orbitals on the oxalato ligand (vide infra).

This structure is broadly similar to that found for $[Cu_2(tacn)_2(\mu\text{-}ox)](ClO_4)_2$ by Zhang et al.,[19] but there are significant differences in that the Cu–O distances in **C2** are slightly longer and give rise to a Cu···Cu separation that is 0.291 Å longer in **C2** than in the tacn counterpart. One reason for this could be that extensive H-bonding involving the secondary nitrogen atoms was found in the tacn complex, which cannot be formed by the alkylated ligand in **C2**.

The overall structure of **C3** is similar to that of **C2**, the main difference being that $BzMe_2tacn$ ligands cap the ends of the complex instead of Me_3tacn (see Figure 4). The tertiary nitrogen atom with the benzyl pendant arm occupies an apical position and, as in **C2**, this Cu–N distance is longer (by 0.24 Å) than the two in the basal plane (see Table 4), and the two apical positions are oriented *trans* with respect to the oxalato bridge. The φ angle (see Figure 7) in **C3** is much larger [12.2(1)°] and the two copper(II) centres are closer to each other [Cu–Cu distance 5.178(11) Å]. A further significant difference is that the oxalato ligand in **C3** binds much more strongly and the bridging unit is more symmetric, viz. all the Cu–O distances [1.9908(11) and 1.9982(11) Å] are identical, while in **C2**, these distances are quite different [2.026(2) and 2.091(2) Å]. In contrast to **C2**, the two Cu–N(tacn) distances in the equatorial plane are identical (av. 2.205 Å), while those in **C2** differ by 0.09 Å (Table 3). It may have been anticipated that the $BzMe_2tacn$ ligand in **C3** would have been more likely to induce structural asymmetry. The more symmetric Cu^{II} coordination sphere allows for a closer approach of the weakly interacting perchlorate counterion [Cu(1)–O(3) distance of 2.648(13) Å is a little shorter than the corresponding bond in **C2**].

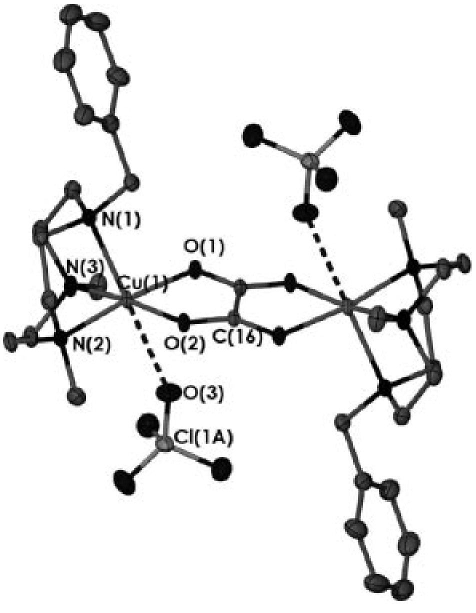

Figure 4. Thermal ellipsoid plot of **C3** (drawn at 50% probability, dashed lines indicate a weak interaction, hydrogen atoms omitted for clarity).

Table 4. Selected bond lengths [Å] and angles [°] for **C3** (esd in parentheses).

Cu(1)···Cu(1)[a]	5.178(1)	O(1)–Cu(1)–O(2)	83.98(4)
Cu(1)–O(1)	1.991(1)	O(1)–Cu(1)–N(2)	173.65(5)
Cu(1)–O(2)	1.998(1)	O(2)–Cu(1)–N(2)	93.43(5)
Cu(1)–N(2)	2.022(1)	O(1)–Cu(1)–N(3)	95.75(5)
Cu(1)–N(3)	2.028(1)	O(2)–Cu(1)–N(3)	172.35(5)
Cu(1)–N(1)	2.265(1)	N(2)–Cu(1)–N(3)	86.05(5)
Cu(1)–O(3)	2.648(1)	O(1)–Cu(1)–N(1)	102.12(5)
O(2)–C(16)	1.257(2)	O(2)–Cu(1)–N(1)	102.38(5)
O(1)–C(16)[a]	1.254(2)	N(2)–Cu(1)–N(1)	84.09(5)
C(16)–O(1)[a]	1.254(2)	N(3)–Cu(1)–N(1)	85.17(5)
C(16)–C(16)[a]	1.538(3)		

Symmetry transformations used to generate equivalent atoms: [a] $-x + 2, -y, -z + 1$.

Magnetic Properties

Variable-temperature magnetic susceptibility studies were carried out on powdered samples of **C2** and **C3** to determine the nature and strength of the magnetic exchange interactions between the copper(II) centres in these oxalato-bridged dinuclear complexes. The measurements were performed in the 4.2–300 K temperature range with an applied field of 1 T. Plots of the magnetic moment vs. temperature for **C2** and **C3** are given in Figures 5 and 6, respectively.

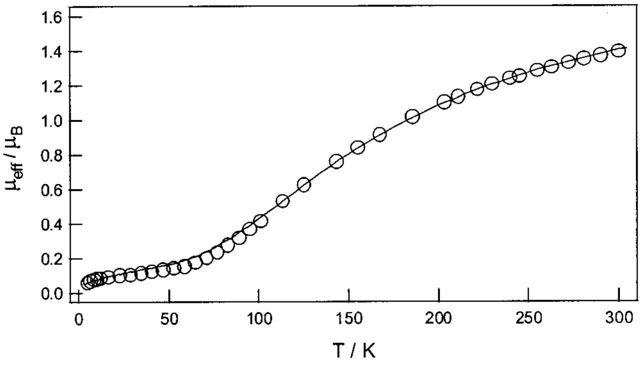

Figure 5. Plot of μ_{eff} (per Cu) vs. temperature for **C2**. The solid line is the best fit using the parameters: g = 2.17, $N\alpha$ = $60 \times 10^{-6}\,cm^3\,mol^{-1}$, J = –159 cm^{-1}, monomer = 0.3%.

Figure 5 shows that the magnetic moment of **C2** decreases substantially from 1.43 μ_B (per Cu) at 300K to 0.08 μ_B at 4.2 K. This is indicative of a strong antiferromagnetic interaction between the Cu^{II} centres. The data were modelled using a $-2J\bar{S}_1 \cdot \bar{S}_2$ Bleaney–Bowers approach,[20] by fitting to the susceptibility Equation (1), where all the sym-

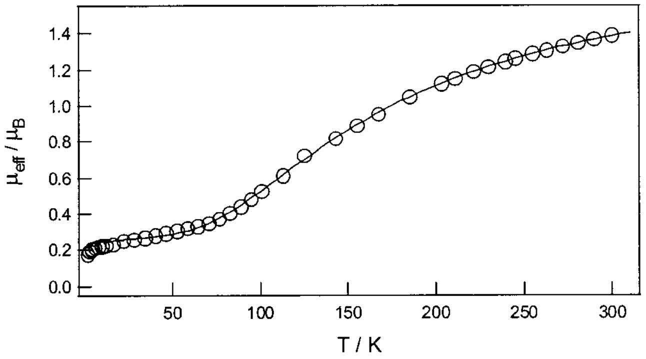

Figure 6. Plot of μ_{eff} (per Cu) vs. temperature for **C3**. The solid line is the best-fit using the parameters: g = 2.03, $N\alpha$ = 60×10^{-6} cm^{3}mol^{-1}, J = –147 cm^{-1}, monomer = 1.8 %.

bols have their usual meaning. The best fit parameters for **C2** are g = 2.17, $N\alpha$ (temperature independent paramagetism) = 60×10^{-6} cm^{3}mol^{-1}, J = –159 cm^{-1}, with a monomer impurity of 0.3 %.

$$\chi_M = \frac{Ng^2\beta^2}{kT}\left[\frac{2}{3+\exp\left(\frac{-2J}{kT}\right)}\right] + N\alpha \qquad (1)$$

For **C3**, the magnetic moment drops from 1.39 μ_B (per Cu) at 300 K to 0.21 μ_B at 4.2 K (Figure 6). This also indicates strong antiferromagnetic coupling. The data were fitted using the same approach as for **C2** to yield the best-fit parameters of g = 2.03, $N\alpha$ = 60×10^{-6} cm^{3}mol^{-1}, J = –147 cm^{-1}, monomer impurity of 1.8 %.

Magnetostructural Correlations

There has been much work aimed at determining how molecular structure influences the extent of magnetic interaction between metal centres with all types of bridging motifs.[1–5,9,10,12,13,15,19,21–25] Until recently, predictions of the extent of magnetic interactions in dinuclear copper(II) complexes have been largely based upon observations of how certain geometrical features influence magnetism. For example, Hoffmann et al.[26] determined that the coupling constant, J, for a d^9 metal complex is given by Equation (2), where $|\varepsilon_S - \varepsilon_A|^2$ is the splitting energy between the singly occupied molecular orbitals and K_{ab}, J_{aa} and J_{ab} are the two-electron integrals involving the localised orthogonal orbitals involved in the magnetic interaction.

$$2J = 2K_{ab} - \frac{|\varepsilon_S - \varepsilon_A|^2}{(J_{aa} - J_{ab})} \qquad (2)$$

Computational studies by Ruiz et al.[8,27] have led to the more general conclusion that the strength of antiferromagnetic coupling in oxalato-bridged dinuclear complexes is determined predominantly by two main geometrical factors: the out-of-plane displacement of the copper ion (h_{Cu}), and the dihedral angle between the plane of the oxalato ligand and the basal coordination plane (φ) (see Figure 7).

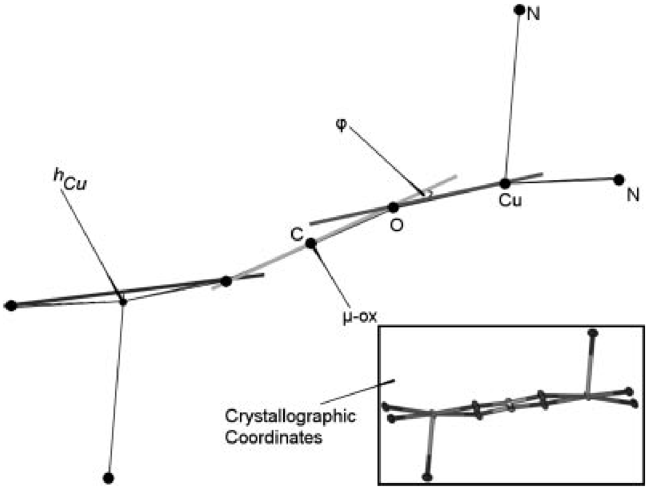

Figure 7. Representation of the core geometry of the complex cation structural motif showing the angle (φ) between the plane of the oxalato ligand and the O–Cu–O plane.

A compilation of structural and magnetic properties of related oxalato-bridged copper(II) complexes can be found in Table 5. Curiously, [Cu$_2$(tacn)$_2$(μ-ox)](ClO$_4$)$_2$, which has

Table 5. Selected magneto-structural parameters for oxalato-bridged Cu^{II} complexes of the type [(L)Cu(μ-ox)Cu(L)]X$_2$.[a]

L	X	φ [°][b]	h_{Cu} [Å][c]	$d_{Cu–Cu}$ [Å]	2J [cm^{-1}]	Ref.
Me$_3$tacn	ClO$_4$	4.8(3)	0.08	5.467(3)	–318	this work
BzMe$_2$tacn	ClO$_4$	12.2(1)	0.12	5.178(11)	–294	this work
tacn	ClO$_4$	1.2/3.1	0.043/0.049	5.176	–41	[19]
phen	NO$_3$	16.9	0.27	5.158(1)	–330	[28]
bdpm	ClO$_4$	2.2	0.3293	5.194	–102	[19]
bipy	NO$_3$	3.2	0.16	5.154(1)	–386	[1]
bipy	ClO$_4$	12.0	0.18	5.150(1)	–376	[12]
bipy	BF$_4$	10.4	0.16	5.144(1)	–378	[12]
dpa	NO$_3$	7.2	0.08	5.22	–305	[24]
tmen	ClO$_4$	8.4	0.18	5.147/5.167	–385.4	[1]
deen	ClO$_4$	3.9	n/r	n/r	–300	[29]
mpz	PF$_6$	13.9	0.24	n/r	–402	[30]
mpz	NO$_3$	2.1	0.06	n/r	–312	[30]
mpz	NO$_3$	n/r	0.12	5.217	–284	[31]
dpp	NO$_3$	7.3	0.16	5.171(1)	–312	[9]
bpz	Cl	4.9	0.10/0.09	5.134(2)	–345	[9]
Pz$_2$CPh$_2$	Cl	20.3	0.39	5.212	–364	[14]
Pz$_2$CPh$_2$	NO$_3$	18.7	0.35	5.161	–344	[14]
Pz$_2$CPh$_2$	ClO$_4$	2.6	0.26	n/r	–424	[14]
Pz$^{3m}{}_2$CPh$_2$	NO$_3$	23.6	0.34	5.178	–378	[14]

[a] Abbreviations: Me$_3$tacn = 1,4,7-trimethyl-1,4,7-triazacyclononane; BzMe$_2$tacn = 1-benzyl-4,7-dimethyl-1,4,7-triazacyclononae, tacn = 1,4,7-triazacyclononane; phen = 1,10-phenanthroline; bdpm = bis(3,5-dimethylpyrazol-1-yl)methane; bipy = 2,2′-bipyridine; dpa = 2,2′-dipyridylamine; tmen = *N*,*N*,*N*′,*N*′-tetramethylethylenediamine; deen = *N*,*N*-diethylethane-1,2-diamine; mpz = 4-methoxy-2-(5-methoxy-3-methylpyrazol-1-yl)-6-methylpyrimidine; dpp = 2,3-bis(2-pyridyl)pyrazine; bpz = 2,2′-bipyrazine; Pz$_2$CPh$_2$ = diphenyldipyrazolylmethane; Pz$^{3m}{}_2$CPh$_2$ = diphenylbis(3-methylpyrazolyl)methane; n/r = not reported. [b] Dihedral angle between the mean oxalato plane and the basal coordination plane. [c] Distance of the copper atom from the basal plane.

a very similar bridging motif to both **C2** and **C3**, exhibits relatively weak antiferromagnetic coupling.[19] Both **C2** and **C3**, which have similar J values, have larger φ and h_{Cu} values than the parent tacn complex but this difference does not account for the large difference in the J value. In [Cu_2(tacn)$_2$(μ-ox)](ClO_4)$_2$, quite strong hydrogen bonding exists between the secondary amine group of the tacn ligand and oxalato oxygen atoms [N–H···O = 2.138(3) Å] on adjacent dinuclear complex units. This could withdraw electron density from the σ-bonding orbitals of the oxalato bridge, hence weakening the strength of orbital overlap with the magnetic orbitals on the copper(II) centre.

The data in Table 5 also indicate that the strength of antiferromagnetic coupling in **C2** and **C3** is similar to that found in many of the other complexes. The strength of the antiferromagnetic coupling in **C2** is of interest as this complex features the longest Cu···Cu distance (by ca. 0.2 Å) reported so far for these types of complexes. However, as can be seen from the collected structural and coupling data, there seems to be no correlation between the extent of coupling and any particular set of geometric parameters. This is clearly highlighted by the fact that **C2** and **C3** have a similar $2J$ value, but have a 7° diffence in the φ angle, and 0.04 Å difference in h_{Cu}.

Conclusions

This work has shown that *N*-alkylation of the tacn macrocycle significantly increases the strength of antiferromagnetic coupling in oxalato-bridged dinuclear copper(II) complexes to the extent that in [Cu_2(Me_3tacn)$_2$(μ-ox)](ClO_4)$_2$ strong coupling has been observed over a Cu···Cu distance (5.46 Å) that is 0.2 Å longer than in any other related oxalato-bridged Cu^{II} complex.

Experimental Section

Materials and Reagents: All solvents and reagents used were of reagent or analytical grade and used as purchased. Distilled H_2O was used throughout. [Cu(Me_3tacn)(OH_2)$_2$](ClO_4)$_2$ (**C1**) was prepared according to Fry et al.[16] 1-Benzyl-4,7-dimethyl-1,4,7-triazacyclononane was prepared according to a previously reported method.[6]

Instrumentation: UV/Vis spectra were recorded in acetonitrile using a Varian Cary 5G spectrophotometer. IR spectra were recorded using a Perkin–Elmer FTIR 1600 series spectrometer at 4.0 cm^{-1} resolution, using KBr discs. CHN microanalyses were carried out by the Campbell Microanalytical Laboratory, University of Otago, New Zealand. Magnetic susceptibilities were measured on samples of ca. 20 mg in mass using a Quantum Design MPMS 5 Squid instrument. Diamagnetic corrections were made for the gelatine capsule sample holder and for ligands using Pascal's constants.

Caution: Although no problems were encountered in this work, transition metal perchlorates are potentially explosive and should be prepared in small quantities and handled with care.

Synthesis of [Cu_2(Me_3tacn)(μ-ox)](ClO_4)$_2$ (C2): A solution of $Na_2C_2O_4$ (0.096 g, 0.70 mmol) in H_2O (5 mL) was added to a solution of [Cu(Me_3tacn)(OH_2)$_2$](ClO_4)$_2$ (0.30 g, 0.64 mmol) in H_2O (10 mL). The resulting solution was heated at reflux for 1 h. The solution was then concentrated to dryness and residues were dissolved in a hot solution of MeOH/EtOH (1:1). The resulting blue solution was then filtered while hot and the filtrate slowly cooled to yield deep-blue crystals that were suitable for X-ray crystallography. Yield: 0.21 g (86%). $C_{20}H_{42}Cl_2Cu_2N_6O_{12}$ (756.58): calcd. C 31.8, H 5.6, N 11.1; found C 32.0, H 5.6, N 11.1. IR (selected bands; KBr disk): ṽ = 2996 (w), 2965 (m), 2924 (s), 1648 (s), 1467 (s), 1352 (m), 1300 (m), 1145 (s), 1078 (br. s), 1015 (s), 1006 (s), 894 (m), 786 (m), 746 (w) cm^{-1}. UV/Vis (MeCN): $\lambda_{\max}$ ($\varepsilon_{\max}$) = 1100 (68), 636 (118), 333 (4160), 282 (11100), 195 (11400 M^{-1} cm^{-1}) nm.

Synthesis of [Cu_2($BzMe_2$tacn)(μ-ox)](ClO_4)$_2$ (C3): 1-Benzyl-4,7-dimethyl-1,4,7-triazacyclononane (0.21 g, 0.85 mmol) was dissolved in MeOH/H_2O (1:1) (10 mL) and a solution of Cu(ClO_4)$_2$·6H_2O (0.32 g, 0.87 mmol) in H_2O (5 mL) was slowly added to this solu-

Table 6. Crystallographic data.

	C1	**C2**	**C3**
Empirical formula	$C_9H_{25}Cl_2CuN_3O_{10}$	$C_{20}H_{42}Cl_2Cu_2N_6O_{12}$	$C_{32}H_{50}Cl_2Cu_2N_6O_{12}$
M [g mol^{-1}]	469.76	756.58	908.78
Crystal system	monoclinic	monoclinic	monclinic
Space group	$P2_1/n$	$C2/c$	$P2_1/n$
a [Å]	8.5463(17)	25.593(5)	7.7961(4)
b [Å]	13.713(3)	7.7096(15)	19.0662(9)
c [Å]	14.741(3)	16.222(3)	13.0878(7)
β [°]	91.08(3)	93.13(3)	99.742(3)
V [Å^3]	1727.2(6)	3196.1(11)	1917.31(17)
Z	4	4	2
T [K]	123(2)	123(2)	123(2)
λ [Å]	0.71073	0.71073	0.71073
D_c [g cm^{-3}]	1.806	1.572	1.574
μ (Mo-K_α) [mm^{-1}]	1.630	1.562	1.317
No. data measured	20597	18296	29838
Unique data (R_{int})	4109 (0.0792)	3583 (0.0507)	6884 (0.0264)
Observed data [$I > 2(\sigma)$I]	3034	2899	5669
Final R_1, wR_2 (obsd. data)	0.0383,[a] 0.0739[b]	0.0462,[a] 0.1075[b]	0.0351,[a] 0.0889[b]
Final R_1, wR_2 (all data)	0.0682, 0.0809	0.0628, 0.1158	0.0470, 0.0960
$\rho_{\min}$, ρ_{max} [e Å^{-3}]	–0.604, 0.481	–0.441, 1.111	–0.869, 0.989

[a] $R = \Sigma(|F_o| - |F_c|)/\Sigma|F_o|$. [b] $R' = [\Sigma w(|F_o| - |F_c|)^2/\Sigma F_o{}^2]^{1/2}$, where $w = [\sigma^2(F_o)]^{-1}$.

tion. The resulting mixture was then stirred at room temperature for 1 h and filtered. A solution of $Na_2C_2O_4$ (0.11 g, 0.84 mmol) in H_2O (5 mL) was added to the filtrate. The mixture was allowed to stand at room temperature and crystals suitable for X-ray diffraction crystallography grew directly from the solution. Yield 0.21 g (54%). $C_{32}H_{50}Cl_2Cu_2N_6O_{12}$ (908.78): calcd. C 42.3, H 5.6, N 9.3; found C 42.6, H 5.6, N 9.4. IR (selected bands; KBr disk): $\tilde{\nu}$ = 2936 (m), 2851 (m), 1654 (s), 1466 (m), 1355 (w), 1315 (w), 1087 (s), 997 (m), 898 (w), 782 (m), 727 (m), 701 (m), 637 (m), 623 (m), 490 (w) cm^{-1}. UV/Vis (MeCN): λ_{max} (ε_{max}) = 1090 (67), 644 (110), 284 (9100 $M^{-1}cm^{-1}$) nm.

X-ray Crystallography: Intensity data for blue crystals of **C1** (0.15 × 0.15 × 0.11 mm), **C2** (0.3 × 0.1 × 0.1 mm) and **C3** (0.30 × 0.10 × 0.09 mm) were measured at 123 K with a Nonius Kappa CCD (Bruker Kappa Apex II for **C3**) fitted with graphite-monochromated Mo-K_α radiation (0. 71073 Å). The data were collected to a maximum 2θ value of 55° (60° for **C3**) and processed using the Bruker–Nonius software. Crystal parameters and details of the data are summarised in Table 6. The structures were solved by direct methods and expanded using standard Fourier routines in the SHELX-97 software package.[32,33] All hydrogen atoms were placed in idealised positions and all non-hydrogen atoms were refined anisotropically. The water hydrogen atoms in **C1** were located on the Fourier difference map but restraints were placed upon them during refinement. The perchlorate anion in **C3** is disordered over two distinct positions, and the chlorine atoms as well as two of the perchlorate oxygen atoms had their site occupancy refined against each other. CCDC-605826 (for **C1**), -605827 (for **C2**) and -605828 (for **C3**) contain the supplementary crystallographic data for this paper. These data can be obtained free of charge from The Cambridge Crystallographic Data Centre via www.ccdc.cam.ac.uk/data_request/cif.

[1] M. Julve, M. Verdaguer, O. Kahn, A. Gleizes, M. Philoche-Levisalles, *Inorg. Chem.* **1983**, *22*, 368.

[2] O. Kahn, *Inorg. Chim. Acta* **1982**, *62*, 3.

[3] O. Kahn, J. Galy, Y. Journaux, J. Jaud, I. Morgenstern-Badarau, *J. Am. Chem. Soc.* **1982**, *104*, 2165.

[4] M. F. Charlot, S. Jeannin, O. Kahn, J. Lucrece-Abaul, *Inorg. Chem.* **1979**, *18*, 1675.

[5] V. H. Crawford, H. W. Richardson, J. R. Wasson, D. J. Hodgson, W. E. Hatfield, *Inorg. Chem.* **1976**, *15*, 2107.

[6] M. J. Belousoff, M. B. Duriska, B. Graham, S. R. Batten, B. Moubaraki, K. S. Murray, L. Spiccia, *Inorg. Chem.* **2006**,*45*, 3746.

[7] H. Hu, Y. Liu, D. Zhang, C. Liu, *Theochem* **2001**, *546*, 73.

[8] E. Ruiz, P. Alemany, S. Alvarez, J. Cano, *J. Am. Chem. Soc.* **1997**, *119*, 1297.

[9] J. Carranza, H. Grove, J. Sletten, F. Lloret, M. Julve, P. E. Kruger, C. Eller, D. P. Rillema, *Eur. J. Inorg. Chem.* **2004**, 4836.

[10] O. Castillo, I. Muga, A. Luque, J. M. Gutierrez-Zorrilla, J. Sertucha, P. Vitoria, P. Roman, *Polyhedron* **1999**, *18*, 1235.

[11] T. R. Felthouse, E. J. Laskowski, D. N. Hendrickson, *Inorg. Chem.* **1977**, *16*, 1077.

[12] A. Gleizes, M. Julve, M. Verdaguer, J. A. Real, J. Faus, X. Solons, *J. Chem. Soc., Dalton Trans.* **1992**, 3209.

[13] P. Gomez-Saiz, J. Garcia-Tojal, M. Maestro, J. Mahia, L. Lezama, T. Rojo, *Eur. J. Inorg. Chem.* **2003**, 2123.

[14] J. L. Shaw, G. T. Yee, G. Wang, D. E. Benson, C. Gokdemir, C. J. Ziegler, *Inorg. Chem.* **2005**, *44*, 5060.

[15] Z. Smekal, J. Kamenicek, P. Klasova, G. Wrzeszcz, Z. Sindelar, P. Kopel, Z. Zak, *Polyhedron* **2002**, *21*, 1203.

[16] F. Fry, A. J. Fischmann, M. J. Belousoff, L. Spiccia, J. Brugger, *Inorg. Chem.* **2005**, *44*, 941.

[17] K. Nakamoto, *Infrared and Raman Spectra of Inorganic and Coordination Compounds*, 4th ed., John Wiley & Sons, New York, **1986**.

[18] F. A. Cotton, G. Wilkinson, C. A. Murillo, M. Bochmann, *Advanced Inorganic Chemistry*, 6th ed., Wiley-Interscience, New York, **1999**.

[19] L. Zhang, B. Wei-Ming, S.-P. Yan, Z.-H. Jiang, D.-Z. Liao, G.-L. Wang, *Polyhedron* **2000**, *19*, 1105.

[20] B. Bleaney, K. D. Bowers, *Proc. R. Soc. London, Ser. A* **1952**, *214*, 451.

[21] Y.-M. Lee, H.-C. Jung, S.-N. Choi, N. H. Hur, *J. Kor. Chem. Soc.* **2000**, *44*, 166.

[22] W.-G. Lu, Y.-F. Pan, C.-H. Peng, *Wuji Huaxue Xuebao* **2005**, *21*, 709.

[23] P. S. Mukherjee, T. K. Maji, S. Koner, G. Rosair, N. R. Chaudhuri, *Ind. J. Chem. Sect. A* **2001**, *40A*, 451.

[24] S. Youngme, N. Chaichit, P. Gunnasoot, P. Kongsaeree, I. Mutikainen, O. Roubeau, J. Reedijk, U. Turpeinen, *Inorg. Chim. Acta* **2003**, *353*, 119.

[25] S. Youngme, P. Gunnasoot, N. Chaichit, C. Pakawatchai, *Transition Met. Chem.* **2004**, *29*, 840.

[26] P. J. Hay, J. C. Thibeault, R. Hoffmann, *J. Am. Chem. Soc.* **1975**, *97*, 4884.

[27] J. Cano, P. Alemany, S. Alvarez, M. Verdaguer, E. Ruiz, *Chem. Eur. J.* **1998**, *4*, 476.

[28] A. Bencini, A. C. Fabretti, C. Zanchini, P. Zanini, *Inorg. Chem.* **1987**, *26*, 1445.

[29] R. Vincente, J. Escuer, J. Ferretjans, H. Stoecklis-Evans, X. Solons, M. Font-Bardia, *J. Chem. Soc., Dalton Trans.* **1997**, 167.

[30] L. Soto, J. Garcia, E. Escriva, J. P. Legros, J. P. Tuchagues, F. Dahan, A. Fuertes, *Inorg. Chem.* **1989**, *28*, 3378.

[31] L. S. Tuero, J. Garcia-Lozano, E. E. Molto, M. B. Borja, F. Dahan, J. P. Tuchagues, J. P. Legros, *J. Chem. Soc., Dalton Trans.* **1991**, 2619.

[32] G. M. Sheldrick, *SHELXL-97*, University of Göttingen, Germany, **1997**.

[33] G. M. Sheldrick, *SHELXS-97*, University of Göttingen, Germany, **1997**.

Received: June 19, 2006